Identification of Metabolism-associated Genes and Construction of a Prognostic Signature in Bladder Cancer

Chengquan Shen
Affiliated Hospital of Medical College Qingdao University
Jing Liu
Affiliated Hospital of Medical College Qingdao University
Liping Wang
Affiliated Hospital of Medical College Qingdao University
Zhijuan Liang
Affiliated Hospital of Medical College Qingdao University
Haitao Niu
Affiliated Hospital of Medical College Qingdao University
Yonghua Wang (doctoryonghua123@sina.com)
Department of Urology, The Affiliated Hospital of Qingdao University, Qingdao, Shandong, China.
https://orcid.org/0000-0002-8861-1003

Primary research

Keywords: bladder cancer, metabolism, TGF-β1, prognosis, TCGA

Posted Date: August 21st, 2020

DOI: https://doi.org/10.21203/rs.3.rs-59450/v1

Version of Record: A version of this preprint was published on November 4th, 2020. See the published version at https://doi.org/10.1186/s12935-020-01627-8.

Abstract

Background

Bladder cancer (BC) is a commonly diagnosed malignant tumor in the urinary system, with a high morbidity and recurrence rate. Current studies indicated that metabolism-associated genes (MAGs) having critical roles in the etiology of BC. The present study aims to identify differentially expressed MAGs and construct a MAGs prognostic risk signature in BC by using The Cancer Genome Atlas (TCGA) database and proteomics data.

Methods

RNA-sequence data from the TCGA database and proteomics were used to identify differentially expressed MAGs and construct a prognostic MAGs signature in BC. Subsequently, survival analysis and nomogram were used to evaluate the prognostic and predictive value of the MAGs model in BC. RNA isolation and reverse transcription-quantitative PCR (RT-qPCR) was further performed to investigate the expression levels of MAGs in BC cell lines and explore the relationship between MAGs and M2 tumor associated macrophages (TAMs) secreted TGF-beta 1 in BC.

Results

A total of 23 differentially expressed MAGs were identified and five MAGs were finally used to construct a MAGs based signature. Survival analysis revealed that the MAGs based signature was closely correlated with the survival outcomes of patients with BC. A nomogram with the MAGs based signature risk score and clinical features also constructed to facilitate the individualized prediction of BC patients. RT-qPCR showed that four MAGs were significantly elevated and the expression levels of three MAGs were positively correlated with M2 TAM secreted TGF-β1 in T24 cells.

Conclusions

Our study identified novel prognostic MAGs and constructed a MAGs based signature, which can be used as an independent signature in evaluating the prognosis of patients with BC. Furthermore, M2 TAMs may promote the expression of three MAGs via TGF-β1 signaling pathway. Further clinical trials and experimental exploration are needed to validate our observations in BC.

Introduction

Bladder cancer (BC) is one of the most malignant and highly aggressive tumors in the urinary system with high recurrence and mortality [1]. The 2015 China cancer statistics showed that BC has led to about 80,500 new cases and 32,900 deaths [2]. In the past few decades, numerous efforts have been made to

develop diagnostic tools and treatments of BC, but the recurrence and mortality rates of BC are still high. Recently, metabolic reprogramming has been considered a novel hallmark of cancer cells [3]. Increased glycolysis under normoxic conditions (Warburg effect), glutamine metabolism, and lipid metabolism are the main characteristics of malignant tumors. Previous studies have indicated that metabolic pathways play critical roles in the occurrence and progression of BC [4–6]. Therefore, it is indispensable to explore more potential reliable and valuable biomarkers, especially metabolism-associated genes (MAGs), to predict disease development and prognosis in BC patients.

In this study, RNA-sequencing (RNA-seq) data from the TCGA database and proteomic data from our samples were used to identify differentially expressed MAGs in BC patients and developed a MAGs based signature, which was significantly related to the prognosis of BC. A prognostic nomogram combined with the MAGs based signature and clinical characteristics was developed to evaluate the clinical predictive value of the MAGs based signature. In addition, the mRNA expression levels and potential mechanisms of five MAGs were further validated in vitro experiments.

Methods

Data collection

RNA-seq expression profiles and clinical information of BC patients were downloaded from the TCGA database (https://tcga-data.nci.nih.gov/tcga/). TCGA cohort contained 414 BC patients, and more detailed clinical characteristics are described in Table 1. The MAGs were collected from the Molecular Signature Database v5.1 (MSigDB).

Table 1
TCGA BC patient characteristics.

Clinical characteristics		Total (414)	%
Age at diagnosis		69 (34–90)	
Gender	Female	109	26.33
	Male	305	73.67
Histologic grade	High Grade	388	93.71
	Low Grade	21	5.07
Stage	I	2	0.48
	II	131	31.64
	III	141	34.06
	IV	136	32.85
T	T0	1	0.24
	T1	3	0.72
	T2	120	28.98
	T3	196	47.34
	T4	59	14.25
M	M0	196	47.34
	M1	11	2.66
N	N0	239	57.73
	N1	47	11.35
	N2	76	18.36
	N3	8	1.93

LC-MS/MS analysis

In the present study, all of the tissue samples were collected from the 10 patients treated with surgical resection, including 10 BC tissues and 10 normal tissues. The 10 patients who underwent laparoscopic radical cystectomy and who did not receive preoperative radiotherapy and chemotherapy. According to the ethical guidelines as required by the Declaration of Helsinki, informed consent was provided by each patient, and the research protocol was approved by the Ethical Committee of the Affiliated Hospital of Qingdao University.

Comparative proteomic profiling is commonly used to LC-MS/MS. In this study, the same method was performed to characterize the variety of proteins in BC samples and normal samples. The process contained protein extraction, trypsin digestion, TMT/iTRAQ Labeling, HPLC Fractionation, LC-MS/MS Analysis, Database Search, and bioinformatic methods. The enrichment of the differentially expressed protein against all identified proteins was detected by two-tailed Fisher's exact test, and protein domains with a corrected p-value < 0.05 were recognized as statistically significant. To further distinguish up- or down-regulated of these proteins in BC, we set the threshold of the ratio between BC and normal samples to 1.2.

Identification of differentially expressed MAGs

The differentially expressed MAGs in the TCGA BC cohort were identified using R software (version R 3.5.1, https://bioconductor.org/packages/release/bioc/) [7]. False discovery rate (FDR) < 0.05 and |log2 fold change (FC)| > 1 were recognized as the cutoff values. We applied heatmap and volcano to exhibit significant differentially expressed MAGs in the TCGA BC cohort. Subsequently, the protein levels of these differentially expressed MAGs were further explored in our BC samples. Boxplot was applied to display MAGs, which were differentially expressed in both mRNA and protein levels. Gene ontology (GO) enrichment analysis and KEGG pathway analysis for differentially expressed MAGs were also performed using the "clusterProfiler" R package.

Construction and evaluation of a MAGs based prognostic risk signature

Univariate Cox regression analysis was performed using the R package "survival" and genes with a significance level of $p < 0.05$ were selected as candidate prognostic MAGs to establish a signature. Multivariate Cox regression analysis was utilized to further establish a prognostic MAGs based signature [8]. The prognostic risk score for each BC patient was calculated as follows: (Coefficient gene 1 × expression of gene 1)+(Coefficient gene 2 × expression of gene 2)+⋯+(Coefficient gene 5 × expression of gene 5). After that, we classified 403 patients into high- and low-risk groups according to the median value of risk score. Kaplan-Meier analysis was used to estimate the significant differences in survival between the high- and low-risk groups. The survival ROC package was used to conduct the receiver operating characteristic curve (ROC). Univariate and multivariate Cox regression analyses were used to assess prognostic significances of the signature and clinical characteristics. In addition, the Wilcoxon signed-rank test was performed to identify the relationship between the MAGs based signature risk score and clinical characteristics.

Development of a nomogram based on MAGs signature and clinical characteristics

Nomogram is applied to predict the survival outcomes of cancer patients and could dynamically monitor the prognosis of patients [9]. Clinical parameters and the MAGs signature risk score were used to

establish a nomogram to evaluate the probability of 1-, 2-, and 3- year OS for BC patients via the R package (https://cran.r-project.org/web/packages/rms/) [10].

Correlation analysis between risk score and immune cell infiltration in BC

Previous studies showed the immune microenvironment of BC, especially immune cell infiltration in tumors, can influence the metabolic levels of BC and further promotes or inhibits the progression of BC. Thus, Tumor Immune Estimation Resource (TIMER), a useful resource for comprehensive analysis of tumor-infiltrating immune cells, was employed to explore the correlations between the signature risk score and immune cell infiltration. The composition of six tumor-infiltrating immune cells subsets (B cells, CD4 + T cells, CD8 + T cells, macrophages, neutrophils, and dendritic cells) was estimate by using the TIMER algorithm. The levels of immune cell infiltration in BC patients were obtained from the TIMER website and the relationship between the signature risk score and six tumor-infiltrating immune cells was performed in R.

RNA isolation and reverse transcription-quantitative PCR

To further validate the mRNA expression levels of five MAGs in BC cell lines, RNA isolation and reverse transcription-quantitative PCR (RT-qPCR) was performed. The T24 and SV-HUC-1 cell lines were supplied by the cell bank of the Chinese Academy of Sciences. The materials used for the cell culture, including the 1640 culture medium, FBS, trypsin, penicillin, and streptomycin, were purchased from Gibco Co. (Grand Island, NY, USA). The total RNA was extracted using Trizol (Takara, code no 9109) according to the manufacturer's recommendations. For the detection of mRNA levels, the total RNA (500 ng) was transcribed into cDNA using a PrimeScript™ RT reagent kit (Perfect Real Time) (Takara, code no RR037A). All the primers were synthesized by Huada Gene (Beijing, China) and the sequences are shown in Table 3. The amplification of cDNAs was conducted with Roche Light Cycler 480II real-time PCR detection system (Roche, Basel, Switzerland). Gene expression was normalized against βactin and relative expression levels of *PLOD1*, *CKB*, *PYGB*, *AKR1B1*, and *PDE5A* were determined by the comparative threshold cycle (Ct) method using the formula $2^{-(\Delta\Delta Ct)}$.

Table 3
Sequences of the primers used for real-time quantitative PCR.

Name of primer	Sequence of primer (5’ to 3’)
PLOD1-F	AAGCCGGAGGACAACCTTTTA
PLOD1-R	GCGAAGAGAATGACCAGATCC
CKB-F	GCTGCGACTTCAGAAGCGA
CKB-R	GGCATGAGGTCGTCGATGG
PYGB-F	AGGTGCGGAAGAGCTTCAAC
PYGB-R	TCGCGCTCGTAGTAGTGCT
AKR1B1-F	TTTTCCCATTGGATGAGTCGG
AKR1B1-R	CCTGGAGATGGTTGAAGTTGG
PDE5A-F	GCAGAGTCCTCGTGCAGATAA
PDE5A-R	GTCTAAGAGGCCGGTCAAATTC

The relationship between M2 TAMs secreted TGF-β1 and five MAGs in BC cell lines.

TIMER analysis indicated that the signature was significantly related to macrophages in BC. Current studies have demonstrated that TGF-beta 1 played an important role in the metabolic programming of the microenvironment of tumors and M2 tumor associated macrophages (TAMs) can secret TGF-β1. Therefore, the relationship between M2 TAM secreted TGF-β1 and five MAGs expression levels were further explored in T24 cell lines. The T24 cells were seeded at $2–10 \times 10^5$ cells/well in 24-well plates for 24 hours and incubated at 37 °C in a humidified atmosphere containing 5% CO2. THP-1 is a human leukemia monocytic cell line, which has been extensively used to study macrophages functions, mechanisms, and signaling pathways [12]. In the present study, THP-1 monocytes were seeded at 2×10^5 cells/well in 24-well plates and were stimulated for 48 h with 100 ng/ml PMA (phorbol-12-myristate-13-acetate) to fully differentiate into macrophages. After that, PMA-differentiated macrophages (M0) were primed with fresh medium supplemented with 20 ng/ml IL-4 for 24 h to the M2 phenotype. Subsequently, M2 TAMs in 24-well plates were cultured with normal 1640 medium (glucose 2,000 mg/ml) or 1ug/ml TGF-β1 antibody (AF-246-NA, Bio-Techne China Co. Ltd.) with 24 h. Then the T24 cells were stimulated with the supernatant of M2 TAMs for 48 hours. The expression levels of five MAGs were investigated by RT-qPCR.

Results

Identification of differentially expressed MAGs in BC

The mRNA expression data of TCGA BC patients were subjected to identify differentially expressed MAGs. We identified 168 MAGs (68 downregulated and 100 upregulated) between 414 BC tissues and 19 normal tissues. Differentially expressed genes and MAGs in the TCGA BC cohort are displayed in volcano (Fig. 1A-B). To investigate the differences in the proteome of these 168 MAGs between BC and normal samples, we collected samples from 10 patients in the Affiliated Hospital of Qingdao University. These samples were processed and analyzed using LC-MS/MS following the process outlined in supplementary Fig. 1. The result showed that the protein levels of 23 MAGs were differentially expressed in BC among these 168 MAGs. Boxplots were used to screen the mRNA and protein levels 23 MAGs in BC (Fig. 1C-D). The detailed information of the protein expression of 23 MAGs in our samples was shown in Supplementary Table 1. To identify the potential mechanisms of these 23 differentially expressed MAGs in BC, we performed GO and KEGG analyses. We found that the most significant GO enriched terms involved in metabolism were amino acid metabolic process, antibiotic metabolic process, organic hydroxy compound catabolic process, alcohol metabolic process, and glycogen catabolic process (BP, biological process); myelin sheath and mitochondrial matrix (CC, cellular component); and lyase activity, oxidoreductase activity cofactor binding, coenzyme binding electron transfer activity, and NAD binding (MF, molecular function) (Fig. 2A). In the KEGG enrichment analysis, the MAGs were primarily correlated with pathways related to arginine and proline metabolism, lysine degradation, glycerolipid metabolism, histidine metabolism, pyruvate metabolism, tryptophan metabolism, ether lipid metabolism, and glycolysis (Fig. 2B).

Identification of prognosis-related MAGs and construction of a MAGs based prognostic signature

By performing univariate Cox regression analysis on 23 MAGs, a total of 5 MAGs were identified to have significant prognostic value in BC ($P < 0.05$) (Fig. 3A). Subsequently, we utilized multivariate Cox regression analysis to construct a prognostic signature, which contained five MAGs, including *PLOD1* (procollagen-lysine,2-oxoglutarate 5-dioxygenase 1), *CKB* (creatine kinase B), *PYGB* (glycogen phosphorylase B), *AKR1B1* (aldo-keto reductase family 1 member B), and *PDE5A* (phosphodiesterase 5A) (Table 2). We further calculated the prognostic risk score for each BC patient as follows: risk score = (0.0049 × expression level of *PLOD1*) + (0.0018 × expression level of *CKB*) + (0.0033 × expression level of *PYGB*) + (0.0031 × expression level of *AKR1B1*) + (0.0486 × expression level of *PDE5A*). Four hundred and three BC patients were subdivided into high-risk and low-risk groups according to the median value of risk score. K-M survival curve analysis showed that the MAGs based signature was closely associated with poor OS (overall survival) ($P = 5.562e-05$), DSS (disease-specific survival) ($P = 4.896e-03$), PFI (progression-free interval) ($P = 2.915e-02$) in BC (Fig. 3B-D). However, the signature risk score was not correlated with the DFI (disease-free interval) ($P = 7.724e-01$) of BC patients (Fig. 3E). ROC curve analysis was used to further measured the predictive performance of the MAGs based signature risk score. The area under the curves (AUCs) for the MAGs signature, age, gender, grade, stage, T, M, N were 0.766, 0.549, 0.436, 0.553, 0.648, 0.623, 0.522, and 0.638, which indicated superior predictive accuracy of the MAGs signature risk score in survival outcomes (Fig. 3F). We further used Univariate and multivariate Cox

regression analyses to assess the prognostic value of the MAGs based signature and clinical features. Univariate Cox regression analysis showed that age, stage, T (tumor), N (node), and risk score were related to the survival of BC patients (Fig. 4G). Subsequently, multivariate Cox regression analysis indicated that the MAGs based signature was an independent prognostic factor for BC ($P < 0.001$, Fig. 4H).

Table 2
Multivariate Cox regression analysis for OS of five MAGs in BC.

Gene name	coef	HR	HR.95L	HR.95H	*P*-value
PLOD1	0.0049	1.0049	0.9999	1.0099	0.0509
CKB	0.0018	1.0018	1.0003	1.0032	0.0173
PYGB	0.0033	1.0033	0.9991	1.0075	0.1259
AKR1B1	0.0031	1.0031	1.0015	1.0046	0.0001
PDE5A	0.0486	1.0498	1.0145	1.0865	0.0054
HR, hazard ratio					

Association between the MAGs signature risk score and clinicopathologic characteristics

The treatment methods for BC patients depend largely on clinical characteristics, and we evaluated whether there was a statistically significant difference between risk score and clinicopathological characteristics. Our study revealed that the MAGs based signature risk score was correlated with the stage ($P = 1.346e-05$), grade ($P = 1.944e-05$), T ($P = 0.004$), M (metastasis) ($P = 0.005$) of BC patients (Fig. 4A-D). However, the risk score was not related to the gender ($P = 0.599$) and N ($P = 0.086$) of BC patients (Fig. 4E-F).

Construction of a prognostic nomogram for BC

To establish a clinically applicable method for monitoring the prognosis of BC patients, we generated a nomogram to predict the survival of BC patients, by combining age, gender, grade, stage, T, N, M with the MAGs based signature risk score. The result showed that the prognostic nomogram could superiorly predict the 1-, 2-, and 3-year survival outcomes of BC patients (Fig. 5).

Correlation analysis between the risk score and immune cell infiltration in BC

To identify the significance of the MAGs based signature in the tumor microenvironment, the relationship between the abundance of six types of tumor-infiltrating immune cells (B cells, CD4 + T cells, CD8 + T cells, neutrophils, macrophages, and dendritic cells) and the IAGs based signature risk score was explored

in BC. The results indicated that the risk score was positively associated with the infiltration of macrophages (*P* = 1.354e-08, Fig. 6A) and dendritic cells (*P* = 6.016e-04, Fig. 6B). However, the risk score was not correlated with the infiltration of B cells, CD4 + T cells, CD8 + T cells, and neutrophils (Fig. 6C-F).

The supernatant of M2 TAMs can promote the expression levels of five MAGs

RNA isolation and reverse transcription-quantitative PCR (RT-qPCR) was further performed to validate the expression levels of five selected MAGs in T24 and SV-HUC-1 cell lines. The results demonstrated significant differences in the expression levels of five MAGs between T24 and SV-HUC-1 cell lines (Fig. 7A). Among these five MAGs, *PLOD1*, *CKB*, *PYGB* were upregulated, *PDE5A* and *AKR1B1* were downregulated in T24 cells. Compared with the unstimulated T24 cells, the expression of five MAGs were significantly elevated in T24 cell lines after stimulated with the supernatant of M2 TAMs (Fig. 7B). In addition, the expression levels *PLOD1*, *CKB*, and *PYGB* were significantly downregulated in T24 cells when stimulated with the low TGF-β1 supernatant of M2 TAMs, which was inhibited the production of TGF-β1 by using TGF-β1 antibody (Fig. 7C).

Discussion

Metabolic alteration in the tumor microenvironment played a vital role in carcinogenesis, progression, and therapeutic resistance of many cancers, especially BC. Previous studies had demonstrated that the alteration of glutamine and glycolytic levels in BC cells could promote the progression of BC [6, 13]. Considering the importance of the metabolic environment in cancer development, it is crucial to identify metabolic-related prognostic biomarkers for BC. In the present study, we identify 23 MAGs, which were differentially expressed in both mRNA and protein levels. GO and KEGG analyses showed that these MAGs were associated with multiple metabolic pathways. In addition, five differentially expressed MAGs (*PLOD1*, *CKB*, *PYGB*, *AKR1B1*, *PDE5A*) were finally used to construct a prognostic signature and survival analysis indicated that high MAGs risk scores were significantly related to the poor OS, DSS, and PFI of BC patients. Subsequently, Cox regression analyses indicated that the MAGs signature was an independent prognostic factor for BC patients and closely related to stage, grade, T, and M. Nomograms have been used to predict the prognosis of patients by incorporating a variety of significant prognostic factors. We established a prognostic nomogram with clinical factors and the MAGs based signature risk score, which can superiorly predict the OS of BC patients. RT-PCR showed that the expression of four MAGs was elevated in T24 cells and M2 TAMs can promote the expression of *PLOD1*, *CKB*, and *PYGB* in T24 cells by secreting TGF-β1. M2 TAM was associated with the progression of tumors and TGF-β1 was closely related to the proliferation, invasion and metastasis of tumors. Therefore, M2 TAMs may influence the metabolic reprogramming in BC by secreting TGF-β1 to promote the recurrence and progression of BC.

Among these MAGs, *PLOD1* encodes lysyl hydroxylases, which are crucial for collagen biosynthesis, cross-linking, and deposition and can promote cancer progression and metastasis [14]. Yamada Y et al.

revealed that overexpression of *PLOD1* was closely related to poor survival and downregulation of *PLOD1* can decrease the progression of BC [15]. *CKB* was participated in metabolic processes involving glycolysis and could serve as a biomarker for predicting tumor progression [16]. However, the precise role of *CKB* in the occurrence and progression of BC has not been well studied. *PYGB* is an enzyme that metabolizes glycogen and can influence the growth and apoptosis of the cancer cell by regulating the NF-κB/Nrf2 signaling pathway [17]. In addition, *PYGB* was associated with the poor prognosis of cancer and can promote the proliferation and invasion of cancer cells by activating Wnt/β-catenin signaling [18–19]. *AKR1B1*, a member of the aldo/keto reductase superfamily, was associated with the poor survival outcomes of cancer and can promote the occurrence and metastasis of cancer by activating epithelial-mesenchymal transition [20]. *PDE5A* was overexpressed in various tumors and inhibition of *PDE5A* can induce apoptosis and attenuate β-catenin-mediated transcription in breast cancer cells [21–23].

Although some of these MAGs have previously been confirmed as prognostic markers for BC, in this study five MAGs, which were identified closely associated with the survival outcomes of BC by bioinformatics methods, were integrated into a MAGs based signature. All these MAGs have participated in the process of metabolic signaling pathways, such as amino acid metabolism, glucose metabolism, and lipid metabolism. Therefore, we suggested that the MAGs based signature can also reflect the metabolic status of patients with BC. However, several limitations should be considered in our research. Firstly, this is a retrospective study. Therefore, we could not obtain complete information, which may lead to bias. Secondly, more samples need to be further confirmed before clinical application and further experimental studies are needed to investigate the potential molecular mechanisms of these MAGs in BC.

In conclusion, our study identified 23 differentially expressed MAGs and established a MAGs based signature, which can be used as an independent signature in evaluating the prognosis of patients with BC. Furthermore, M2 TAMs may promote the expression of *PLOD1*, *CKB*, and *PYGB* via the TGF-β1 signaling pathway. Further clinical trials and experimental exploration are needed to validate our observations in BC.

Declarations

Ethics approval and consent to participate

The study was approved by the ethics committee of the affiliated hospital of Qingdao University, and the written informed consent was obtained from all patients.

Funding

This work was supported by the National Natural Science Foundation of China (No. 81972378, 81101932).

Authors' contributions

Chengquan Shen: Conceptualization, Methodology, Writing - original draft. Jing Liu and Zhijuan Liang: Data curation. Liping Wang: Software. Haitao Niu: Supervision. Yonghua Wang: Writing - review & editing.

Availability of data and material

The data used to support the findings of this study is included in the article, and the data are available from the corresponding author upon request.

Consent for publication

Not applicable.

Competing interests

The authors declare that they have no conflict of interest.

Acknowledgments

No.

References

1. Antoni S, Ferlay J, Soerjomataram I, Znaor A, Jemal A, Bray F. European urology. 2017 Jan;71(1):96–108. doi: 10.1016/j.eururo.2016.06.010.
2. 2. Chen W, Zheng R, Baade PD, Zhang S, Zeng H, Bray F, Jemal A, Yu XQ, He J. Cancer statistics in China, 2015. CA Cancer J Clin. 2016;66(2):115–32. doi:10.3322/caac.21338.
3. Hanahan D, Weinberg RA. Hallmarks of cancer: the next generation. Cell. 2011;144(5):646–74. doi:10.1016/j.cell.2011.02.013.
4. Massari F, Ciccarese C, Santoni M, Iacovelli R, Mazzucchelli R, Piva F, Scarpelli M, Berardi R, Tortora G, Lopez-Beltran A, Cheng L, Montironi R. Metabolic phenotype of bladder cancer. Cancer Treat Rev. 2016;45:46–57. doi:10.1016/j.ctrv.2016.03.005.
5. Cheng S, Wang G, Wang Y, Cai L, Qian K, Ju L, Liu X, Xiao Y, Wang X. Fatty acid oxidation inhibitor etomoxir suppresses tumor progression and induces cell cycle arrest via PPARγ-mediated pathway in bladder cancer. Clin Sci (Lond). 2019;133(15):1745–58. doi:10.1042/CS20190587.
6. 10.1042/BSR20182372
   Zhou Q, Zhan H, Lin F, Liu Y, Yang K, Gao Q, Ding M, Liu Y, Huang W, Cai Z. LincRNA-p21 suppresses glutamine catabolism and bladder cancer cell growth through inhibiting glutaminase expression. Biosci Rep. 2019 Apr 12;39(4):BSR20182372. doi: 10.1042/BSR20182372.
7. Robinson MD, McCarthy DJ, Smyth GK. edgeR: a Bioconductor package for differential expression analysis of digital gene expression data. Bioinformatics. 2010;26(1):139–40. doi:10.1093/bioinformatics/btp616.

8. Tibshirani R. The lasso method for variable selection in the Cox model. Stat Med. 1997;16(4):385–395. doi:10.1002/(sici)1097-0258(19970228)16:4<385::aid-sim380>3.0.co;2-3
9. Iasonos A, Schrag D, Raj GV, Panageas KS. How to build and interpret a nomogram for cancer prognosis. J Clin Oncol. 2008;26(8):1364–70. doi:10.1200/JCO.2007.12.9791.
10. Qian Z, Li Y, Fan X, Zhang C, Wang Y, Jiang T, Liu X. Prognostic value of a microRNA signature as a novel biomarker in patients with lower-grade gliomas. J Neurooncol. 2018;137(1):127–37. doi:10.1007/s11060-017-2704-5.
11. Min AKT, Mimura K, Nakajima S, Okayama H, Saito K, Sakamoto W, Fujita S, Endo H, Saito M, Saze Z, Momma T, Ohki S, Kono K. Therapeutic potential of anti-VEGF receptor 2 therapy targeting for M2-tumor-associated macrophages in colorectal cancer. Cancer Immunol Immunother. 2020 Jul 23. doi:10.1007/s00262-020-02676-8.
12. Chanput W, Mes JJ, Wichers HJ. THP-1 cell line: an in vitro cell model for immune modulation approach. Int Immunopharmacol. 2014 Nov;23(1):37–45. doi:10.1016/j.intimp.2014.08.002.
13. 10.1016/j.yexcr.2015.04.007
Conde VR, Oliveira PF, Nunes AR, Rocha CS, Ramalhosa E, Pereira JA, Alves MG, Silva BM. The progression from a lower to a higher invasive stage of bladder cancer is associated with severe alterations in glucose and pyruvate metabolism. Exp Cell Res. 2015 Jul 1;335(1):91 – 8. doi: 10.1016/j.yexcr.2015.04.007.
14. Qi Y, Xu R. Roles of PLODs in Collagen Synthesis and Cancer Progression. Front Cell Dev Biol. 2018 Jun 28;6:66. doi: 10.3389/fcell.2018.00066.
15. Yamada Y, Kato M, Arai T, Sanada H, Uchida A, Misono S, Sakamoto S, Komiya A, Ichikawa T, Seki N. Aberrantly expressed PLOD1 promotes cancer aggressiveness in bladder cancer: a potential prognostic marker and therapeutic target. Mol Oncol. 2019 Sep;13(9):1898–912. doi:10.1002/1878-0261.12532.
16. 10.1371/journal.pone.0140492
Mello AA, Leal MF, Rey JA, Pinto GR, Lamarão LM, Montenegro RC, Alves AP, Assumpção PP, Borges Bdo N, Smith MC, Burbano RR. Deregulated Expression of SRC, LYN and CKB Kinases by DNA Methylation and Its Potential Role in Gastric Cancer Invasiveness and Metastasis. PLoS One. 2015 Oct 13;10(10):e0140492. doi: 10.1371/journal.pone.0140492.
17. Wang Z, Han G, Liu Q, Zhang W, Wang J. Silencing of PYGB suppresses growth and promotes the apoptosis of prostate cancer cells via the NF–κB/Nrf2 signaling pathway. Mol Med Rep. 2018 Oct;18(4):3800–3808. doi: 10.3892/mmr.2018.9388.
18. Zhou Y, Jin Z, Wang C. Glycogen phosphorylase B promotes ovarian cancer progression via Wnt/β-catenin signaling and is regulated by miR-133a-3p. Biomed Pharmacother. 2019 Dec;120:109449. doi: 10.1016/j.biopha.2019.109449.
19. Xiao L, Wang W, Huangfu Q, Tao H, Zhang J. PYGB facilitates cell proliferation and invasion in non-small cell lung cancer through activating Wnt/β-catenin signaling. Biochem Cell Biol. 2020 Mar 19. doi:10.1139/bcb-2019-0445.

20. Wu X, Li X, Fu Q, Cao Q, Chen X, Wang M, Yu J, Long J, Yao J, Liu H, Wang D, Liao R, Dong C. AKR1B1 promotes basal-like breast cancer progression by a positive feedback loop that activates the EMT program. J Exp Med. 2017 Apr;214(4)(3):1065–79. doi:10.1084/jem.20160903.
21. Murata T, Shimizu K, Watanabe Y, Morita H, Sekida M, Tagawa T. Expression and role of phosphodiesterase 5 in human malignant melanoma cell line. Anticancer Res. 2010 Feb;30(2):355–8.
22. Sponziello M, Verrienti A, Rosignolo F, De Rose RF, Pecce V, Maggisano V, Durante C, Bulotta S, Damante G, Giacomelli L, Di Gioia CR, Filetti S, Russo D, Celano M. PDE5 expression in human thyroid tumors and effects of PDE5 inhibitors on growth and migration of cancer cells. Endocrine. 2015 Nov;50(2):434–41. doi:10.1007/s12020-015-0586-x.
23. Tinsley HN, Gary BD, Keeton AB, Lu W, Li Y, Piazza GA. Inhibition of PDE5 by sulindac sulfide selectively induces apoptosis and attenuates oncogenic Wnt/β-catenin-mediated transcription in human breast tumor cells. Cancer Prev Res (Phila). 2011 Aug;4(8):1275–84. doi:10.1158/1940-6207.CAPR-11-0095.

Figures

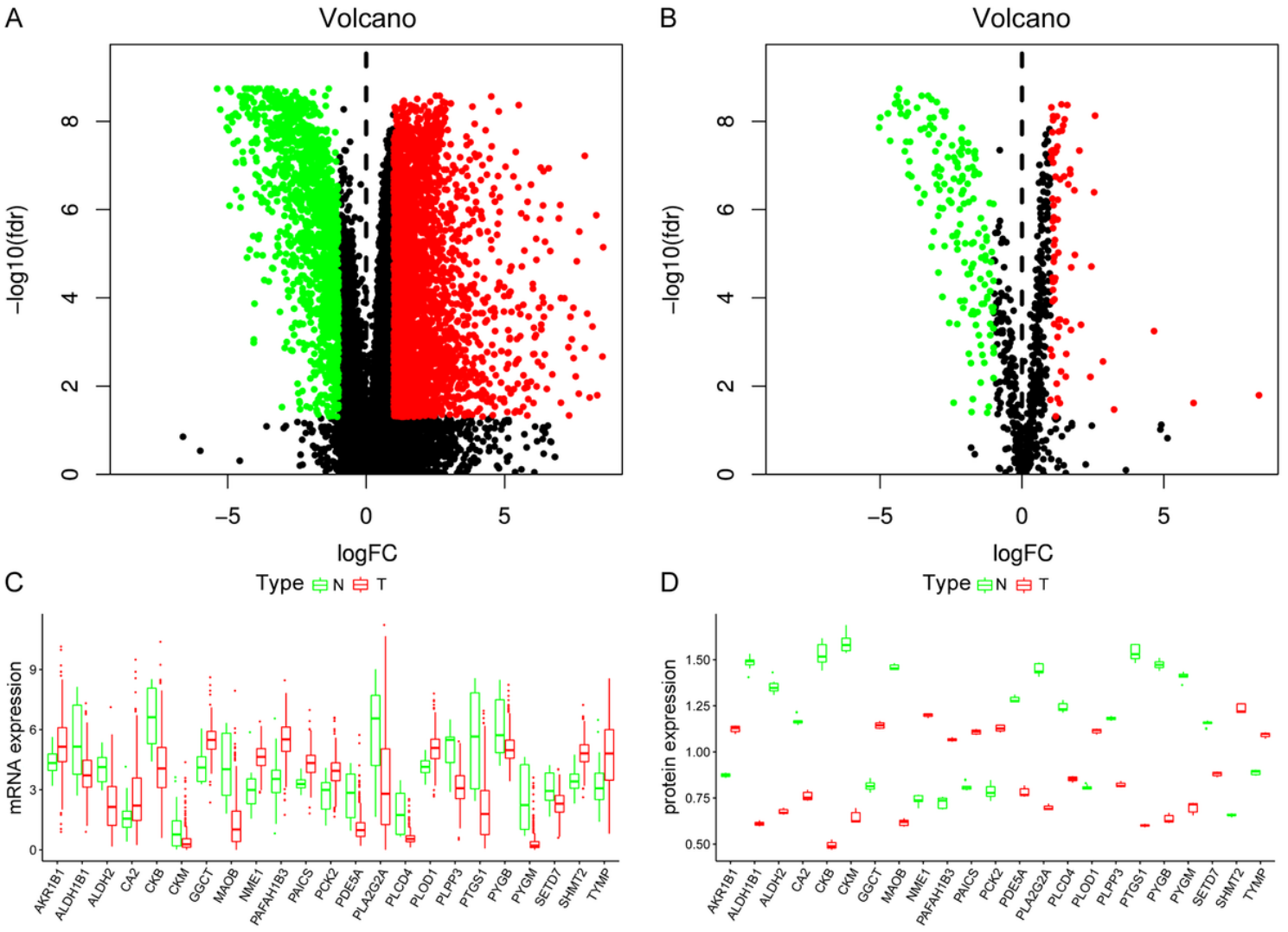

Figure 1

(A)Heatmap and (B)volcano plotof differentially expressed MAGs in BC and normal samples. The red plots represent upregulated genes, and the gene dots represent downregulated genes.(C)Boxplot of the mRNA levels of 23MAGs in the TCGA BC cohort. (D) Boxplot of protein levels of 23 MAGs in our BC tissue samples.

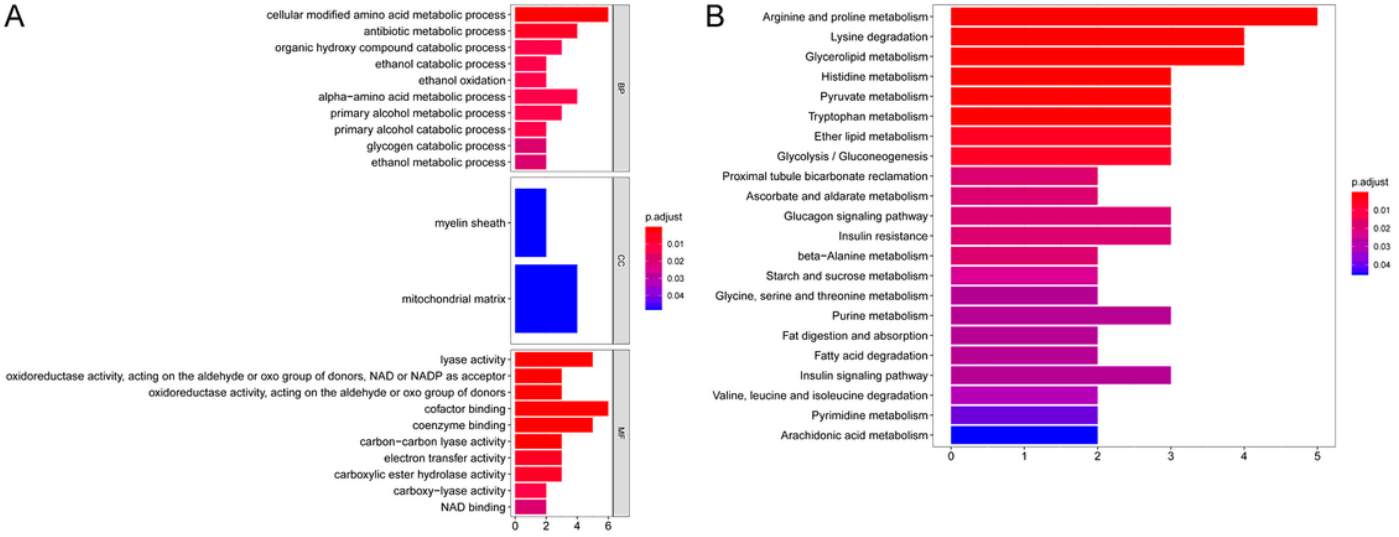

Figure 2

GO and KEGG analyses of differentially expressed MAGs. Heatmap exhibited the enriched GO terms across the differentially expressed MAGs (A). Heatmap exhibited the enriched KEGG pathways across the differentially expressed MAGs(B).

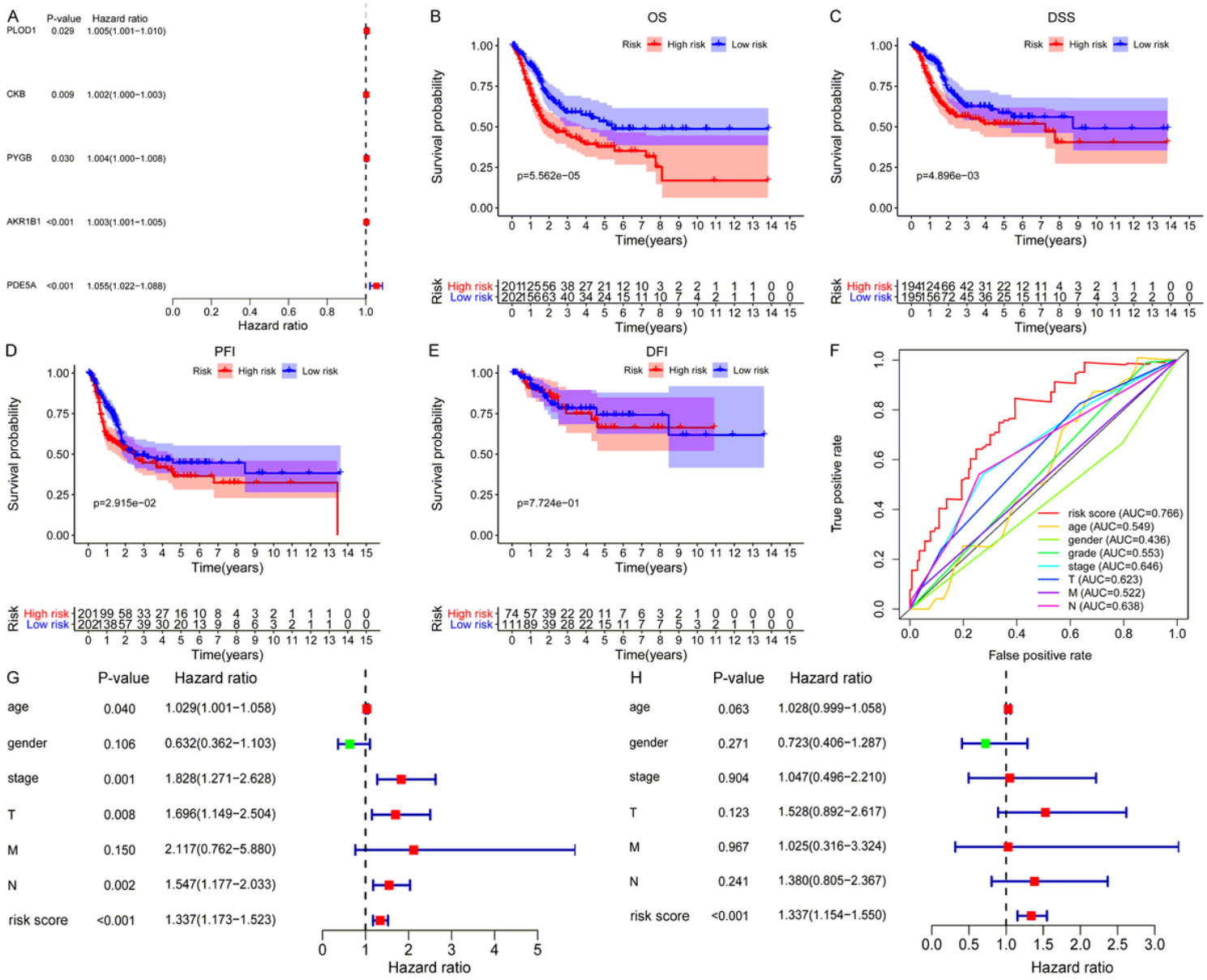

Figure 3

Construction of a MAGs based signature to predict the prognosis of ACC.(A)Univariate Cox regression analysis showed that five MAGs are closely associated with the OS of BC patients. (B-D)Kaplan-Meier curves revealed that the high-risk group had significantly shorter overall survival (OS), disease-specific survival (DSS), and progression-free interval (PFI) compared with the low-risk group. (E) However, the signature was not associated with disease-free interval (DFI). (F) ROC curves showed that the area under the curves (AUCs) of the risk score,age, gender, grade, stage, T, M, and N were 0.766, 0.549, 0.436, 0.553, 0.646, 0.623, 0.522 and 0.638. (G)Univariate Cox regression analysis showed that age, stage, T, N,and risk score were significantly related to the survival of BC patients. (H)Multivariate Cox regression analysis demonstrated that the signature could serve as an independent prognostic predictor for BC patients.

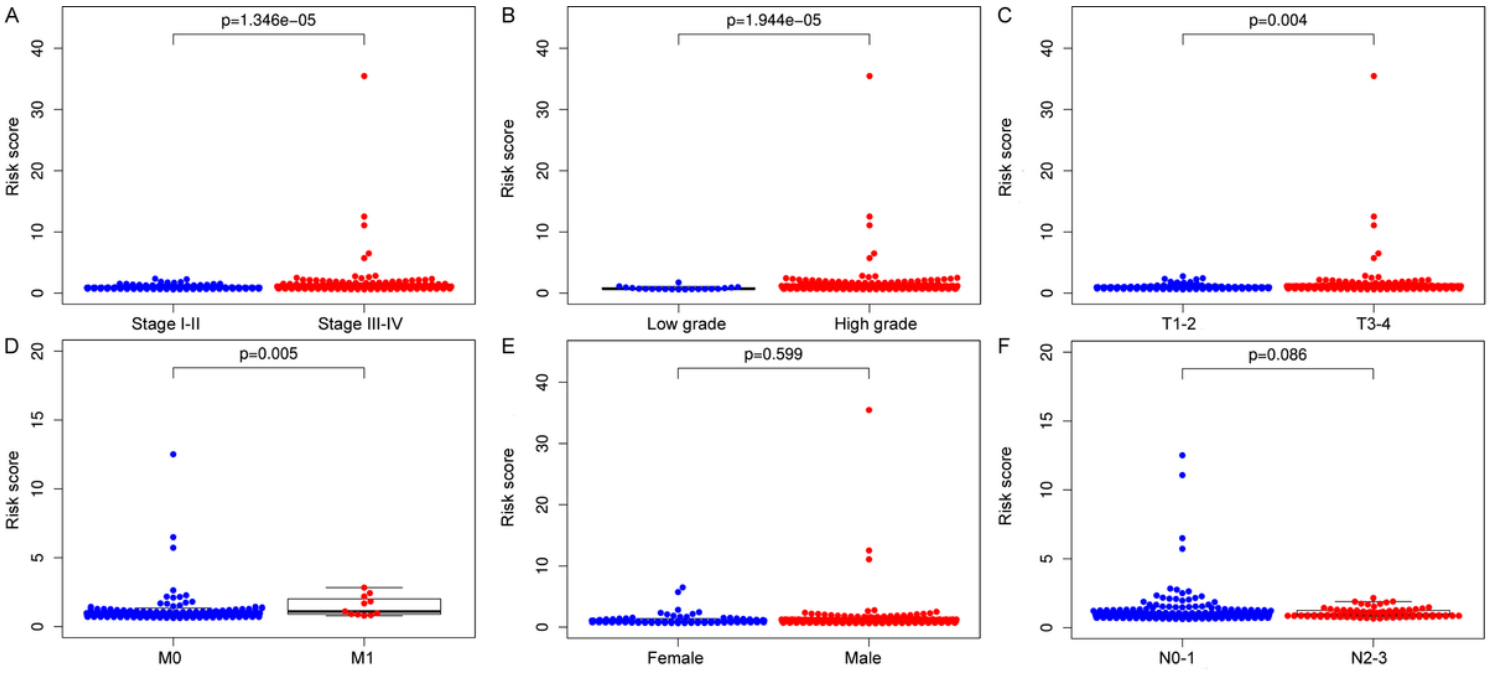

Figure 4

The relationship between the MAGs signature risk score and clinicopathological characteristics.(A-D)The MAGs signature risk score was associated with thestage, grade, T, and M of BC. (E-F)However, the risk score was not related to the gender and N of BC.

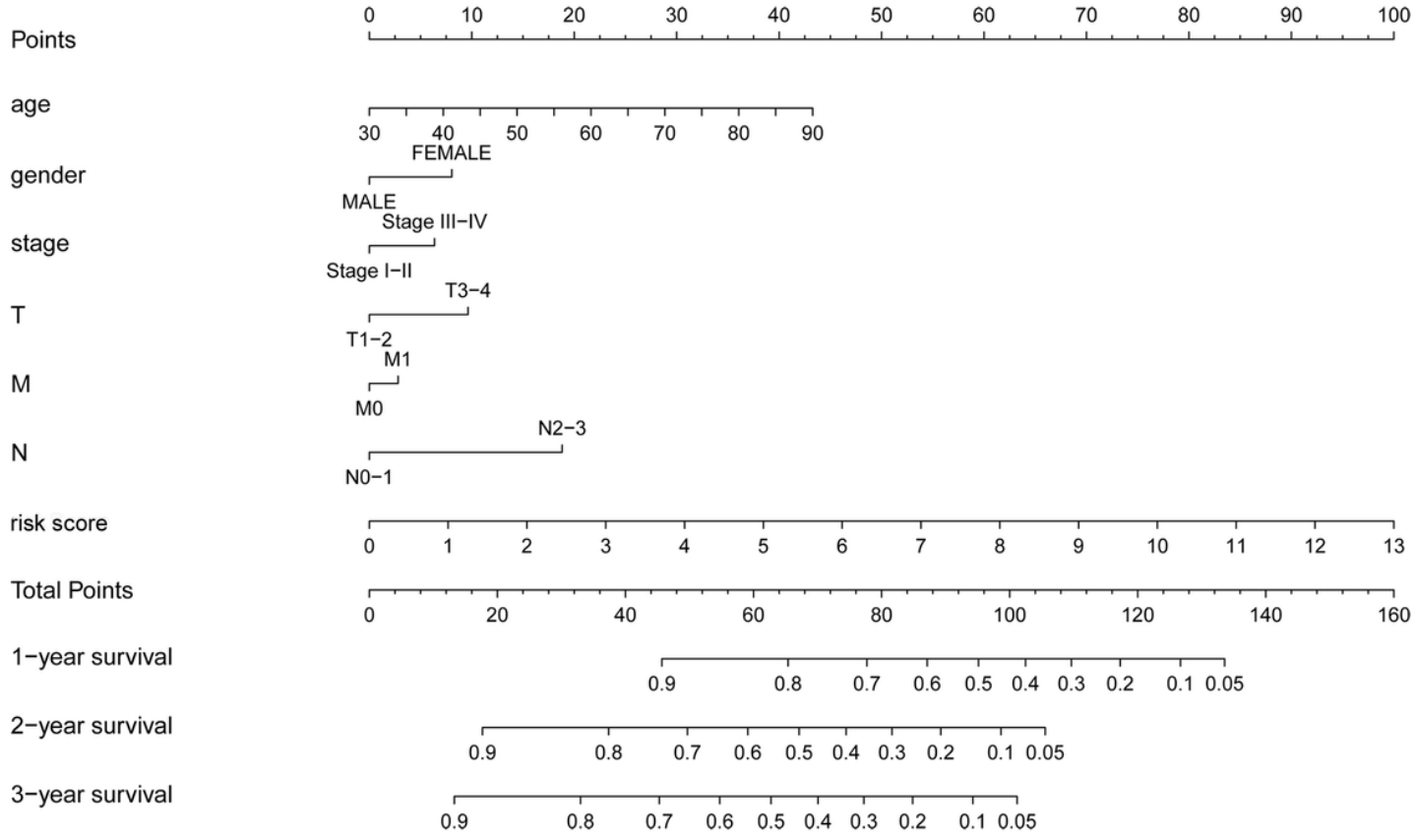

Figure 5

A nomogram with clinical features and MAGs signature risk score for BC. The nomogram could superiorly predict 1-, 2-, and 3-year OS of BC patients.

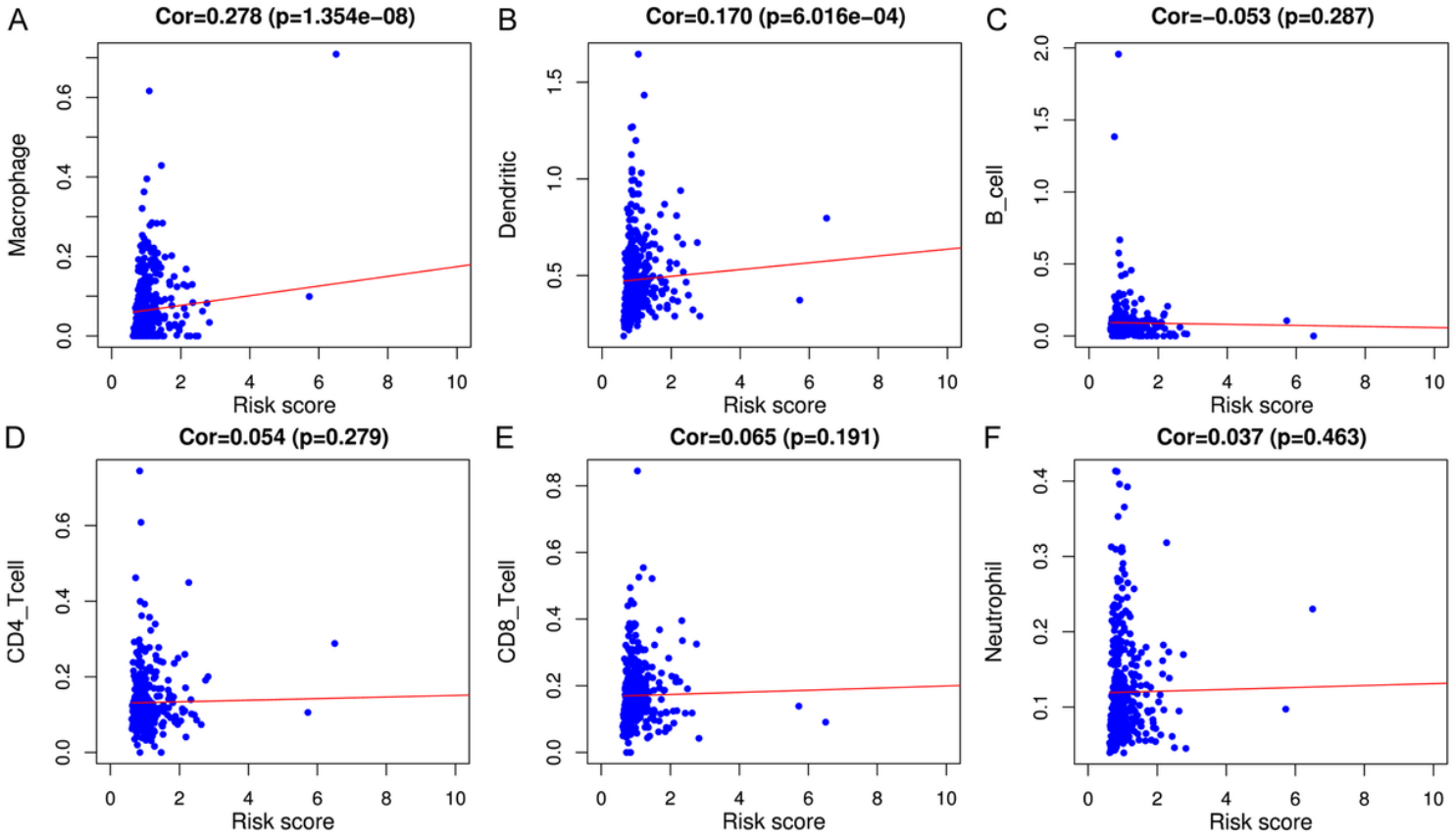

Figure 6

Correlation analysis between the risk score and immune cell infiltration in BC. (A-B) The risk score was positively associated with the infiltration of macrophages and dendritic cells. (C-F) However, the risk score was not correlated with the infiltration of B cells, CD4+ T cells, CD8+ T cells, and neutrophils.

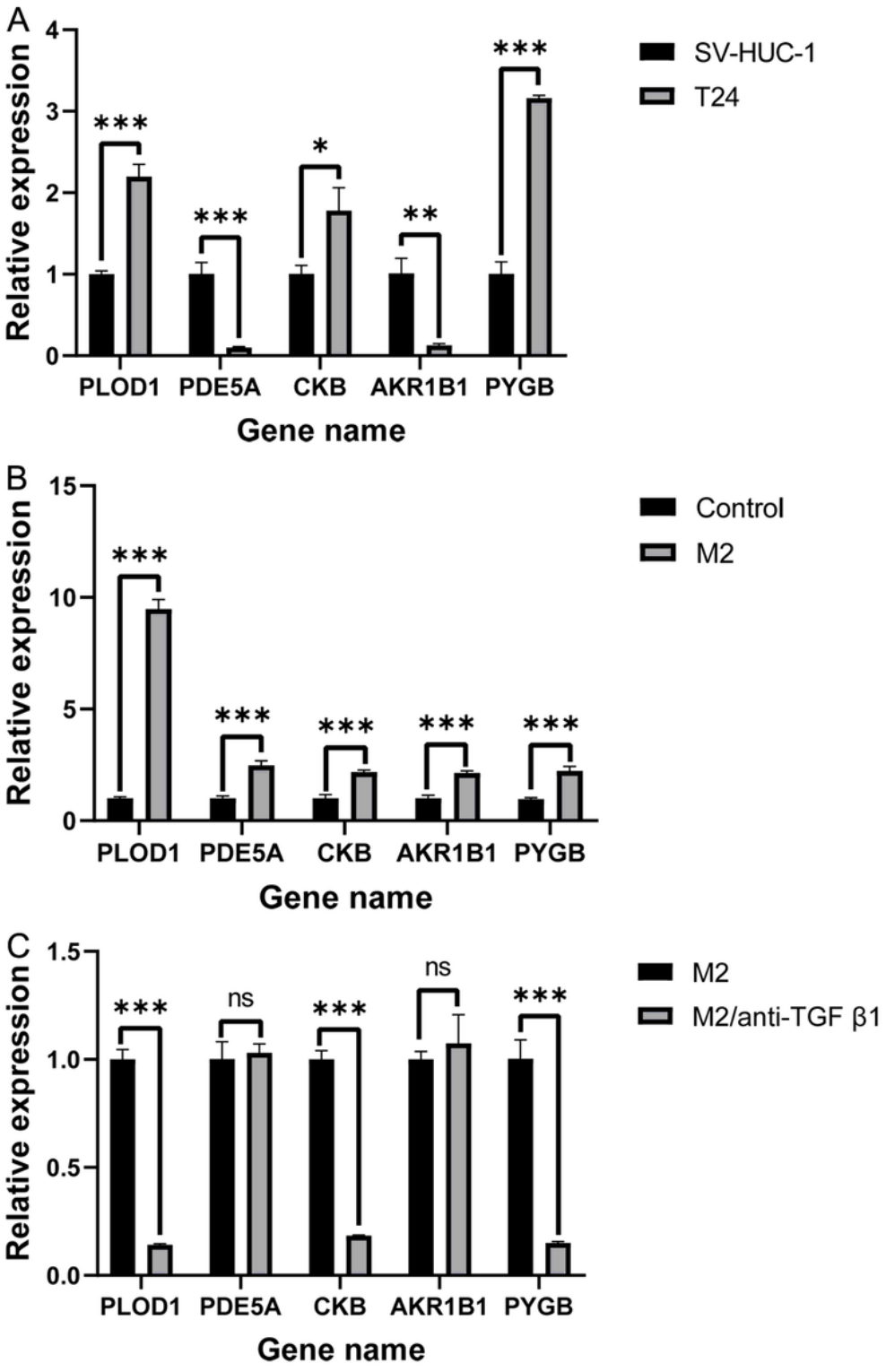

Figure 7

RT-PCR validation of three m6A RNA regulators in ACC and normal tissues. (A) The significant differences in the expression levels of five MAGs between T24 and SV-HUC-1 cell lines. Among these five MAGs, PLOD1, CKB, PYGB were upregulated, PDE5A and AKR1B1 were downregulated in T24 cells. (B) Compared with the unstimulated T24 cells, the expression of five MAGs were significantly elevated in T24 cell lines after stimulated with the supernatant of M2 TAMs. (C) The expression levels PLOD1, CKB, and

PYGB were significantly downregulated in T24 cells when stimulated with the low TGF-β1supernatant of M2 TAMs, which was inhibited the production of TGF-β1 by using TGF-β1 antibody.

Supplementary Files

This is a list of supplementary files associated with this preprint. Click to download.

- supplementary2.docx
- supplementary1.tif